# Ionic and Free Solvent Motion in Poly(azure A) Studied by ac-Electrogravimetry

**ARTICLE** *in* THE JOURNAL OF PHYSICAL CHEMISTRY C · MAY 2011

Impact Factor: 4.77 · DOI: 10.1021/jp2018204



**5 AUTHORS**, INCLUDING:

José Juan García-Jareño
University of Valencia
**126** PUBLICATIONS **1,641** CITATIONS

SEE PROFILE

THE JOURNAL OF PHYSICAL CHEMISTRY C

ARTICLE

pubs.acs.org/JPCC

# Ionic and Free Solvent Motion in Poly(azure A) Studied by *ac*-Electrogravimetry

J. Agrisuelas,[*,†,§] C. Gabrielli,[†,‡] J. J. García-Jareño,[§] H. Perrot,[†,‡] and F. Vicente[§]

[†]CNRS, UPR 15 du CNRS, Laboratoire Interfaces et Systèmes Electrochimiques-LISE, 4, place Jussieu, 75252 Paris, France

[‡]UPMC, Université Pierre et Marie Curie, Laboratoire Interfaces et Systèmes Electrochimiques-LISE, 4, place Jussieu, 75252 Paris, France

[§]Departament de Química Física, Universitat de València, C/Dr Moliner, 50, 46100, Burjassot, València, Spain

**ABSTRACT:** This work is focused on the mechanistic aspects of the redox behavior of poly(azure A) taking advantage of the controlled modulation of their oxidation states by *ac*-electrogravimetry. The originality of this technique is its ability to discriminate between cation and anion involved in the charge compensation process and the accompanying free solvent transfer, directly or indirectly. Two processes were proposed where the faster ionic exchange is considered to be the participation of the anion species acting as counterions whereas the slower one is related to the proton transfer. The proton is implied as reactants for the two electroactive sites identified in the polymer chain, the intermonomeric amino links and the aromatic rings. The *ac*-electrogravimetry technique was used to study the kinetic aspects of the transfer of proton ($H^+$), anion ($NO_3^-$ or $Cl^-$), and free solvent in $KNO_3$ and KCl aqueous solutions.

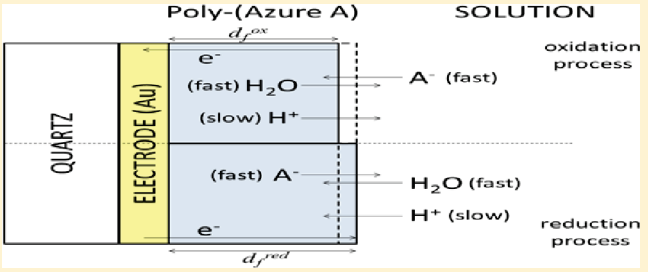


## 1. INTRODUCTION

Intrinsically conducting polymers (ICPs) have been the subject of many research efforts during the past few years.[1−8] The ease of electrogenerating mixed ionic/electronic conducting polymers on different kind of conducting materials was of special interest in technologies for electrochromic devices,[9,10] photogalvanic cells,[11] artificial muscles,[12,13] light-emitting electrochemical cells,[14,15] biosensors,[16−22] and biofuel-cell-based devices,[23,24] among others.

The physical−chemical properties of ICPs are directly linked to the oxidation state of their active sites, which can be controlled by electrochemical oxidation/reduction processes. During the electrochemical reactions occurring in the polymer in the course of its redox switching, several processes may occur: electron transfer between the electrode and the polymer, electron or ion transfer in the polymer, and ion/free solvent transfer between the solution and the polymer. The understanding of such processes related to the charge compensation mechanism is not yet accomplished but is considered as essential. In addition, the apparent kinetics is controlled by the slowest of these processes.

During many years, the electrochemical processes of this kind of polymer have been studied by means of classical electrochemical techniques.[25−27] In the most recent past 10 years, a new technique has been developed:[28−33] *ac*-electrogravimetry. This technique couples electrochemical impedance spectroscopy (EIS) with mass impedance spectroscopy (MIS) using a fast electrochemical quartz crystal microbalance (EQCM) which provides simultaneously the electrochemical impedance, $\Delta E/\Delta I(\omega)$, and a mass/potential transfer function, $\Delta m/\Delta E(\omega)$. The originality of this technique is its ability to discriminate between cation and anion transfers involved in the charge compensation process. Gabrielli et al. have already explained in details the theory of *ac*-electrogravimetry,[34−37] and actually, they are improving this technique.[38]

The polymer of azure A, a phenothiazine (Figure 1), is a particular group of this kind of polymer which belongs to the polyaniline-like group.[39−44] Recent works have shown that an ion exchange based on two processes (one faster and another slower) is a suitable model for the electrochemical reactions of the poly(azure A) (PAA).[45,46] The fast ionic exchange was assumed to be due to the participation of anionic species acting as counterions whereas the slow process is related to protons which could be implied as reactants in the protonation/deprotonation process of the electroactive sites. This dual participation takes place in the two different electroactive sites previously identified in the polymer by spectroscopy:[47] the intermonomeric amino links like the polyaniline formed during the polymerization process and the unchanged aromatic rings shown in Figure 1. The aim of this work is focused on understanding the interactions of ions and free solvent in both sites taking advantage of the controlled modulation of their oxidation states by *ac*-electrogravimetry. For this purpose, two different aqueous solutions ($KNO_3$ 0.5 M and KCl 0.5 M) were used. In this manner, the size of the anion was changed by keeping the other parameters constant.

**Received:** February 24, 2011
**Revised:** April 13, 2011
**Published:** May 13, 2011

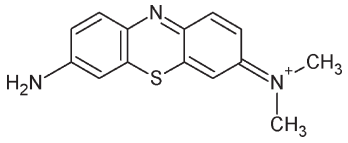

**Figure 1.** Structure of the *N*-(7-amino-3*H*-phenothiazin-3-ylidene)-*N*-methylmethanaminium or azure A.

## 2. *AC*-ELECTROGRAVIMETRY THEORY

At the polymer/electrolyte interface, the ion exchange phenomena are modified when a small sine wave potential perturbation, $\Delta E$, is applied. In this approach, justified previously,[31,34] only the ionic and free solvent transfers are taken into account as the rate-limiting steps. The equation describing the insertion/expulsion law characterizing the species transfer at the polymer/electrolyte interface is

$$\frac{\Delta C_i}{\Delta E}(\omega) = \frac{-G_i}{(j\omega)^{\alpha_i} + K_i/d_f} \quad (1)$$

where $i$ is related to an anion "a", a cation "c", or the free solvent "s"; $C_i$ is the concentration of the species "$i$" in the polymer; $\omega$ is the pulsation equal to $2\pi f$, where $f$ is the perturbation frequency; $d_f$ is the polymer thickness; $G_i$ and $K_i$ are the partial derivatives of the flux with respect to the concentration and potential ($G_i = (\partial J_i/\partial E)_{C_i}$ and $K_i = (\partial J_i/\partial C_i)_E$ where $J_i$ is the flux of the species "$i$" crossing the polymer/electrolyte interface). This model depicts a perfect loop when $\alpha_i = 1$ whereas sometimes the experimental results show depressed loops. Using a constant phase element ($\alpha_i < 1$) instead of a first-order time constant ($\alpha_i = 1$) eliminates this discrepancy in the model.

On the basis of the same model and according to eq 1, the theoretical electrochemical impedance, $\Delta E/\Delta I(\omega)$, is also obtained

$$\frac{\Delta E}{\Delta I}(\omega) = \frac{1}{j\omega C_{dl} + j\omega F \Sigma_{i=a,c}\left[\dfrac{G_i}{(j\omega)^{\alpha_i} + K_i/d_f}\right]} \quad (2)$$

where $K_i/d_f$ can be considered as an apparent parameter $K'_i$ when the thickness of the polymer is unknown and $C_{dl}$ is the polymer/solution double layer capacity.

Another transfer function can be experimentally calculated to obtain complementary information, the charge/potential transfer function, $\Delta q/\Delta E(\omega)$, which gives the number of different charged species participating in the electrochemical processes

$$\frac{\Delta q}{\Delta E}(\omega) = \frac{1}{j\omega}\frac{\Delta I}{\Delta E}(\omega) - C_{dl} \quad (3)$$

and by using eq 1, this theoretical transfer function is equal to

$$\frac{\Delta q}{\Delta E}(\omega) = F\sum_{i=a,c}\frac{G_i}{(j\omega)^{\alpha_i} + K_i/d_f} \quad (4)$$

where $F$ is the Faraday constant.

Finally, from eq 1, the mass/potential transfer function, $\Delta m/\Delta E(\omega)$, is easily deduced

$$\frac{\Delta m}{\Delta E}(\omega) = \sum_{i=a,c,s}\delta_i m_i\frac{G_i}{(j\omega)^{\alpha_i} + K_i/d_f} \quad (5)$$

where $m_i$ is the molar mass of the charged or noncharged species involved in the electrochemical process and $\delta_i$ only reaches values of $+1$ or $-1$. $\delta_a = +1$ indicates that the mass decreases if the polymer is reduced; therefore, the anion is the counterion involved in such an electrochemical process. In this case, eq 5 describes a low- frequency loop in the first quadrant (upper right quadrant of a crossed *XY* plot). On the contrary, if a cation exchange takes place $\delta_c = -1$ and the mass impedance spectrum appears in the third quadrant (bottom left quadrant of a crossed *XY* plot).[32,34]

## 3. EXPERIMENTAL SECTION

The polymer deposition was controlled by cyclic voltammetry (CV) and was carried out in a three-electrode cell, where the reference electrode was saturated calomel electrode (SCE, Tacussel XR 600), the counter electrode was a platinum grid, and the working electrode was a circular gold electrode patterned on a 9 MHz quartz crystal resonator (TEMEX, France) controlled by an Autolab PGSTAT302 potentiostat/galvanostat. All solutions were freshly prepared with bidistilled water. The polymerization solution was $KNO_3$ 0.5 M (Normapur, analytical reagent) and azure A $5 \times 10^{-4}$ M (Sigma), with a pH value around 5. The studied polymer was formed through 600 voltammetric cycles between $-0.6$ V and $+1.0$ V versus SCE with a 100 mV $s^{-1}$ scan rate. After that, the modified electrodes were cycled in the previous voltammetric conditions in $KNO_3$ 0.5 M solutions free of oxygen (at pH = 5) until repetitive voltammograms were obtained (200 cycles), in order to clean the polymer of the residual monomers absorbed and/or to electropolymerize the free units.

The *ac*-electrogravimetric experiments with the resultant polymer were performed in $KNO_3$ 0.5 M and, after, in KCl 0.5 M (Normapur, analytical reagent) with a pH value around 5. For this purpose, a lab-made oscillator acted as a microbalance coupled with a four channel frequency response analyzer (FRA, Solartron 1254) and a potentiostat (SOTELEM-PGSTAT Z1). The EQCM was used under dynamic regime; the modified working electrode was polarized at a selected potential, and a sinusoidal small amplitude potential perturbation (10 mV rms) was superimposed. The microbalance frequency change, $\Delta f_m$, corresponding to the mass response, $\Delta m$, of the modified working electrode, was measured simultaneously with the alternating current response, $\Delta I$, of the electrochemical system through a frequency voltage converter. The resulting signals were sent to the four channels FRA, which allowed the electrogravimetric transfer function, $\Delta m/\Delta E(\omega)$ and the electrochemical impedance, $\Delta E/\Delta I(\omega)$, to be simultaneously obtained at a given potential. The fitting of the experimental data was carried out by means of an optimized version of the Levenberg−Marquardt method for minimization the functions in Mathcad v.14. This procedure allowed the parameters of eqs 7 and 8 to be found.

## 4. RESULTS

The electrogenerated PAA polymer was electrochemically oxidized and reduced using cyclic voltammetry. By means of the EQCM, the changes of mass during the cycle can be also recorded and two zones can be observed (Figure 2a). At the potentials below 0 V, the mass decreases in the oxidation sense and it increases in the reduction sense. Above 0 V, the mass behavior is completely contrary. From the experimental values of mass and current, the use of values of the instantaneous mass/electrical charge ratio at each applied potential prove especially useful in the analysis of the stoichiometry of the electrochemical reactions.[48] The molar mass of the charged species, $m_i$, involved

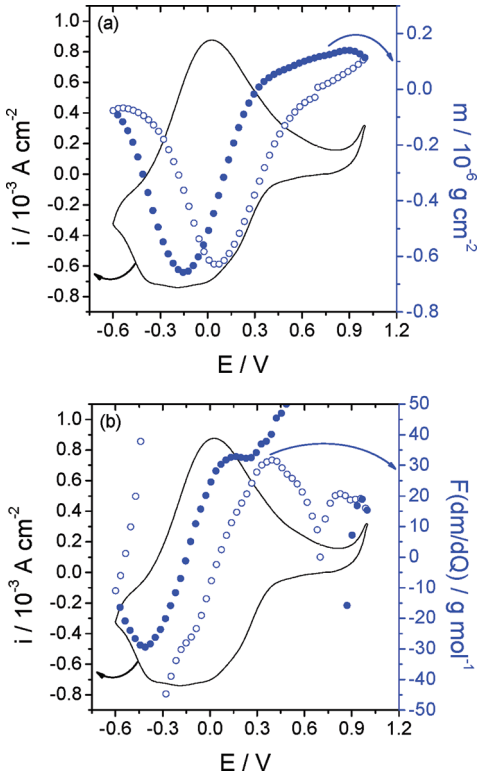


**Figure 2.** (a) Cyclic voltammogram and increments of mass performed to 100 mV $s^{-1}$ and (b) calculated $F(dm/dQ)$ function vs potential of the PAA gold modified electrode in $KNO_3$ 0.5 M at pH = 5 in absence of monomer. Open circles (○) draw the oxidation sense, and filled circles (●) are the reduction sense.

in the electrochemical process can be easily estimated by using the following equation:

$$m_i = F\left(\frac{dm}{dQ}\right) = F\left(\frac{dm/dt}{dQ/dt}\right) = F\left(\frac{dm/dt}{i}\right) \qquad (6)$$

The sign of this function indicates whether charge balance in the polymer during electrochemical reactions takes place by the participation of cations (negative) or anions (positive). However, there are other factors that should be considered in the analysis of this function such as the participation of water molecules that could leave or enter the polymer during the electrochemical reactions associated or not to the ion transfer, or the existence of other reactions that could take place in the outer medium and that do not imply a mass change but a current passes through the electrode.

Following the potential scan between −0.3 and 0.3 V, the molar mass determined for the exchanged species varies between 40 and −30 g $mol^{-1}$, as shown from Figure 2b. It indicates certainly a mixed contribution of anions and cations without excluding the participation of the free solvent. The $F(dm/dQ)$ values smaller than the molecular mass of the $NO_3^-$ ion present in the solution indicate the participation of some cation ($H^+$, $H_3O^+$) or free solvent in the charge-mass balance at positive potentials. The transfer of $K^+$ is not considered since the values of $F(dm/dQ)$ must be even lower. In the negative range of potentials, the $F(dm/dQ)$ values reach −30 g $mol^{-1}$ which is not the molar mass of the cations in solution ($H^+$, $H_3O^+$, $K^+$). Moreover, it is also important to consider the transfer of free solvent. These results are in analogy with the similar poly(neutral red) polymer.[48,49] This point underlines the limitation of the cyclic electrogravimetry technique where only one scan rate was used for a large exploration of the potential. These mass variations were therefore not quantitatively exploited here as *ac*-electrogravimetry experiments reported hereafter are much more powerful to establish a comprehensive understanding of ions and free solvent transfers taking place during insertion/expulsion processes.[50]

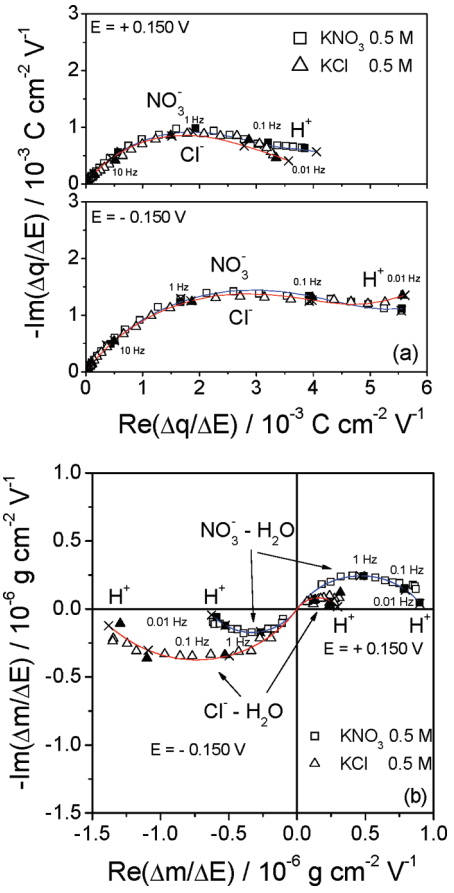


**Figure 3.** (a) Charge/potential transfer function, $\Delta q/\Delta E(\omega)$, and (b) electrogravimetric transfer function, $\Delta m/\Delta E(\omega)$, at $E = +0.150$ V and $E = -0.150$ V vs SCE in $KNO_3$ 0.5 M and KCl 0.5 M solutions at pH = 5. The continuous lines are the theoretical curves calculated from eqs 7 and 8.

*ac*-Electrogravimetry experiments were carried out in $KNO_3$ 0.5 M and KCl 0.5 M. Figure 3 shows the two experimental transfer functions: $\Delta q/\Delta E(\omega)$ and $\Delta m/\Delta E(\omega)$ at $E = +0.150$ V and $E = -0.150$ V versus SCE. In the same graphs, the theoretical curves are also represented using the theoretical transfer functions in eqs 7 and 8, respectively:

$$\frac{\Delta q}{\Delta E}(\omega) = F\left(\frac{G_c}{(j\omega)^{\alpha_c} + K_c'} + \frac{G_a}{(j\omega)^{\alpha_a} + K_a'}\right) \qquad (7)$$

$$\frac{\Delta m}{\Delta E}(\omega) = \delta_c m_c \frac{G_c}{(j\omega)^{\alpha_c} + K_c'} + \delta_a m_a \frac{G_a}{(j\omega)^{\alpha_a} + K_a'} + \delta_s m_s \frac{G_s}{(j\omega)^{\alpha_s} + K_s'} \qquad (8)$$

In this model, an apparent $K'_i$ is obtained since the thickness of the polymer is unknown and the estimation can fall systematically


dx.doi.org/10.1021/jp2018204 |J. Phys. Chem. C 2011, 115, 11132–11139

in error. On the other hand, the constant phase element was fixed ($\alpha_i = 0.6$) considering the nonuniformity of the thickness of the polymer.[51,52] In addition, the transfer direction and molar mass ($\delta_i m_i$) of the considered ions is also known, $\delta_{H^+} m_{H^+} = -1$ g mol$^{-1}$, $\delta_{NO_3^-} m_{NO_3^-} = +62$ g mol$^{-1}$, and $\delta_{Cl^-} m_{Cl^-} = +35.5$ g mol$^{-1}$. Thus, the number of the free parameters are reduced which facilitates the fittings. The first transfer function, $\Delta q/\Delta E(\omega)$ (Figure 3a), exhibits a depressed loop where two transfers can be identified: one fast and one slow.[46] The contribution of the mass transfer function, $\Delta m/\Delta E(\omega)$, allows the participation of cations and anions to be discerned (Figure 3b).[34] Moreover, the coupled motion of the free solvent contributes to the transfer of the mass but has no contribution in the charge transfer measurements. The depressed loop in the first quadrant indicates a decrease (increase) of mass during the reduction (oxidation) process generally at the positive potentials. On the contrary, an increase (decrease) of mass during the reduction (oxidation) takes place for negative potentials; consequently, a depressed loop in the third quadrant is observed. These results are in accordance with the results of the $F(dm/dQ)$ function of Figure 2. In the model proposed in this work, a good correlation was obtained for both functions by considering that the fast process occurring in the high frequency range is associated to the anions ($NO_3^-$ or $Cl^-$), and the slow process occurring at low frequencies to the protons ($H^+$). Moreover, the free solvent has the same transfer direction as the protons ($\delta_{H_2O} m_{H_2O} = -18$ g mol$^{-1}$). This model is in accordance with the previous studies.[45] The anion transfer should be mainly implied in the charge balance, and the proton transfer could follow a Grotthuss mechanism where the transfer is achieved through the hopping of protons between donor and acceptor amine groups.[53] This hopping effect should imply a slower transfer of protons only observed at low frequencies.

The kinetic parameter $G_i$ from eq 7 has been interpreted as the inverse of a charge transfer resistance at the polymer/solution interface or, in other models, mathematical equivalents, $1/FG_i = R_{ct}$. By analogy, this parameter from eq 8 is the inverse of a mass transfer resistance and refers to the rate/easiness of insertion/expulsion of species "$i$" into the polymer during the redox processes.[45,46,49] It can be approximated by

$$G_i = \frac{G_{i,\max}}{\cosh\left[\frac{B_i(E - E_i^{\circ\prime})}{2}\right]} \quad i = \text{a, c, s} \qquad (9)$$

In this equation, $E$ is the applied potential, $E_i^{\circ\prime}$ is the formal potential for the redox process, and $B_i = nF/RT$, where $n$ is the number of electrons involved in this process. $G_{i,\max}$ is the value of $G_i$ at the formal potential $E_i^{\circ\prime}$. $B_i \approx 40$ V$^{-1}$ at 298 K indicates the participation of one electron ($n = 1$) during the insertion of species "$i$" into the polymer in the redox process without the influence of other factors.[34,54] Equation 9 corresponds to a peak-shaped function and is very useful for characterizing a redox process when more than one process is observed.

In previous works, two electroactive sites with different molecular structures were identified by vis−NIR spectroscopy with different formal potential.[46,47] On the one hand, the aromatic ring of the monomer remains intact after the polymerization and preserves the redox activity in the polymeric lattice. On the other hand, new links between the monomers of the azure A are formed during the polymerization; they are supposed to have a molecular structure similar to the links formed in polyaniline.[55] These new links have also a redox activity and, therefore, add a new type of electroactive site in the polymer lattice of PAA which is observed at the more positive potentials with respect to the redox reaction of rings. In this work, two overlapped processes can be proposed for $G_{NO_3^-}$ and $G_{H_2O,NO_3^-}$ (Figure 4a), $G_{Cl^-}$ and $G_{H_2O,Cl^-}$ (Figure 4b), and $G_{H^+,NO_3^-}$ and $G_{H^+,Cl^-}$ (Figure 4c) where $G_{i,NO_3^-}$ and $G_{i,Cl^-}$–$G_{i,Cl^-}$ indicate the quantity

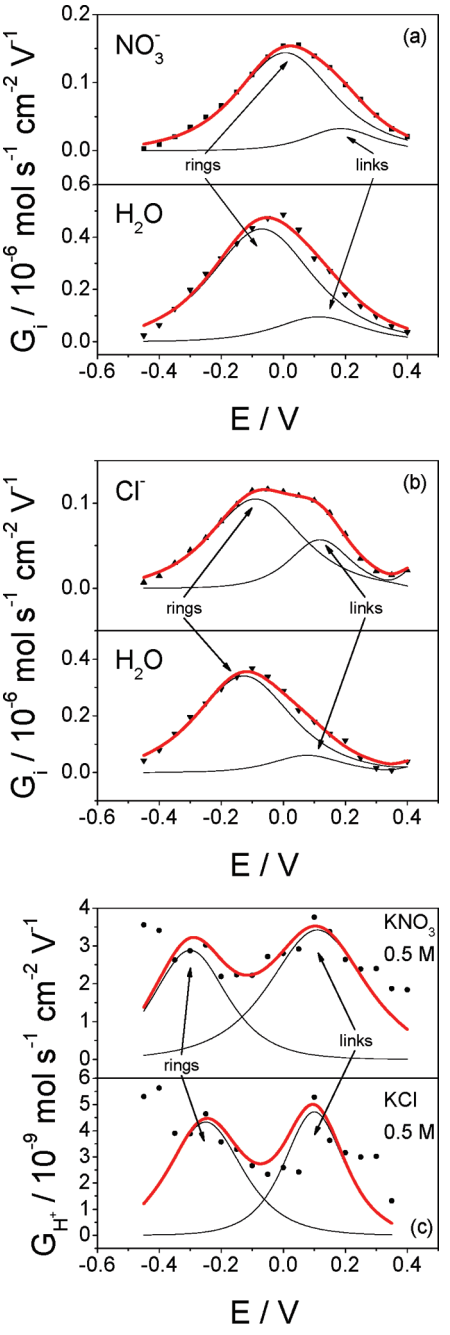


**Figure 4.** Change of the kinetic parameter with respect to the concentration, $G_i$, at different polarization potentials (a) for the $NO_3^-$ ion and $H_2O$ in $KNO_3$ 0.5 M solution, (b) for the $Cl^-$ ion and $H_2O$ in KCl 0.5 M solution, and (c) for the $H^+$ ion (upper) in $KNO_3$ 0.5 M solution and (lower) in KCl 0.5 M solution at pH = 5 obtained by fitting $\Delta q/\Delta E(\omega)$ and $\Delta m/\Delta E(\omega)$ with the theoretical functions, eqs 7 and 8, respectively. The continuous thin lines are the simulated curves of $G_i$ of eq 9 using the parameters in Table 1, and the continuous thick lines are the sum of the individual simulated curves.


dx.doi.org/10.1021/jp2018204 |J. Phys. Chem. C 2011, 115, 11132–11139

**Table 1. Parameters Used in the Simulated Curves of $G_i$ in Equation 9 from Data of Figure 4 for Both Solutions[a]**

| | "links" process | | | "rings" process | | |
|---|---|---|---|---|---|---|
| "$i$" species[b] | $G_{i,max}$, mol s$^{-1}$ cm$^{-2}$ V$^{-1}$ | $B_i$, V$^{-1}$ | $E_i^{o\prime}$, V | $G_{i,max}$, mol s$^{-1}$ cm$^{-2}$ V$^{-1}$ | $B_i$, V$^{-1}$ | $E_i^{o\prime}$, V |
| *$H^+$ | $3 \times 10^{-9}$ | 15 | 0.110 | $3 \times 10^{-9}$ | 20 | −0.300 |
| *$NO_3^-$ | $3 \times 10^{-8}$ | 22 | 0.186 | $15 \times 10^{-8}$ | 15 | 0.007 |
| *$H_2O$ | $10 \times 10^{-8}$ | 17 | 0.115 | $44 \times 10^{-8}$ | 14 | −0.069 |
| **$H^+$ | $5 \times 10^{-9}$ | 25 | 0.100 | $4 \times 10^{-9}$ | 20 | −0.250 |
| **$Cl^-$ | $6 \times 10^{-8}$ | 25 | 0.119 | $11 \times 10^{-8}$ | 16 | −0.089 |
| **$H_2O$ | $6 \times 10^{-8}$ | 21 | 0.077 | $35 \times 10^{-8}$ | 15 | −0.126 |

[a] "Links" process refers to the intermonomeric link redox reactions, and "rings" process is the aromatic ring redox reactions. [b] One asterisk indicates from $KNO_3$ 0.5 M, and two asterisks indicate from KCl 0.5 M aqueous solutions.

$G_i$ in $KNO_3$ and KCl media, respectively: the "links" process for the electrochemical redox reactions of the intermonomeric links and the "rings" process for the electrochemical redox reactions of the aromatic rings. In the range of potentials where the "links" process takes place, the mass of PAA decreases when the polymer is reduced (loop in the first quadrant from Figure 3b). At the more negative potentials, the "rings" process takes place and coincides with an increase of mass when the polymer is reduced (loop in the third quadrant from Figure 3b).

For each simulated process, the characteristic parameters of the transfer of the three species are summarized in Table 1. The $E_i^{o\prime}$ of the anion transfer is placed at the more positive potential than the $E_i^{o\prime}$ of the free solvent transfer and the $H^+$ ion transfer. Among them, the free solvent transfer is the easier transferred (between 6 and $44 \times 10^{-8}$ mol s$^{-1}$ cm$^{-2}$ V$^{-1}$), the next is the anion (between 3 and $15 \times 10^{-8}$ mol s$^{-1}$ cm$^{-2}$ V$^{-1}$) and finally the proton (between 3 and $5 \times 10^{-9}$ mol s$^{-1}$ cm$^{-2}$ V$^{-1}$). As it can be seen, the insertion/expulsion of the $H^+$ ion is the more difficult in comparison with the other species in spite of the smallest size of this cation. By comparing between processes, the transfer of both the anion ($NO_3^-$ or $Cl^-$) and free solvent is always easier during the "rings" process than during the "links" process. On the contrary, this difference is not observed for the $H^+$ ions.

The parameter $B_i$ reaches values between 14 and 25 V$^{-1}$ for all species transfers in both processes (Table 1). The lower values than 40 V$^{-1}$ could be due to stronger interactions between the randomly distributed oxidized and reduced sites during the redox reactions assuming a Frumkin-type isotherm.[56,57] In this work, the 600 voltammetric cycles of polymerization with 100 mV s$^{-1}$ result in a high amount of polymer on the electrode; therefore, the probability of the interactions is increased. In previous works,[45,46] the values of $B_i$ are close to 40 V$^{-1}$ when the amount of deposited polymer is smaller. In this manner, the parameter $B_i$ may be considered like an indirect measurement of the interactions between the electroactive sites.

The variation of the apparent derivative of the flux over the concentration at a constant potential, $K_i'$, at different polarization potentials is presented in Figure 5a for the $KNO_3$ solution and in Figure 5b for the KCl solution. The maximum $K'_{NO_3^-}$ is reached around 0.1 V, and this rate is located between both the $E_i^{o\prime}$ of the $NO_3^-$ ion transfer above that identified (Table 1). On the other hand, the $K'_{Cl^-}$ shows two fastest transfers at potentials very close to the formal potentials found with $G_{Cl^-}$ for both characterized processes of the PAA polymer in KCl solution (Table 1), one around 0.15 V and other around −0.05 V.

Great differences in the values of the $K'_i$ are found between the anion and free solvent transfer which are very similar compared

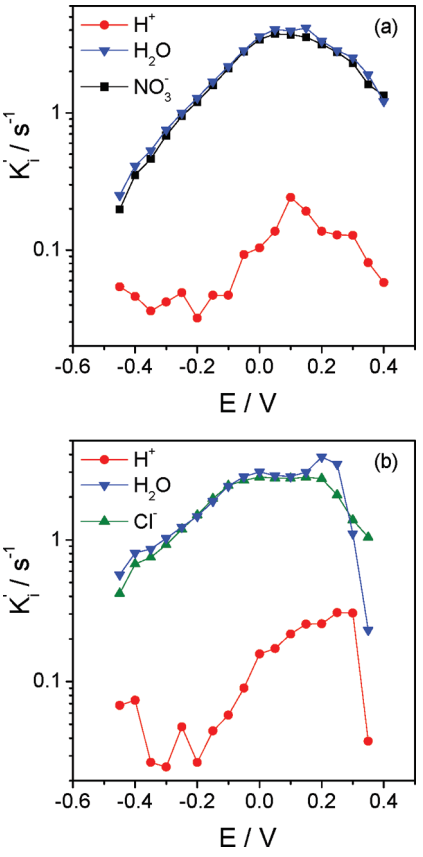


**Figure 5.** Changes of the apparent kinetic parameter, $K'_i$, at different polarization potentials in (a) $KNO_3$ 0.5 M solution and (b) KCl 0.5 M solution at pH = 5 obtained by fitting $\Delta q/\Delta E(\omega)$ and $\Delta m/\Delta E(\omega)$ with the theoretical functions, eqs 7 and 8, respectively.

to the proton transfer. In $KNO_3$ solutions, the rate constants for the free solvent and the $NO_3^-$ ion transfers are between 0.2 and 4 s$^{-1}$. In KCl solution, these values for the anion and free solvent transfers are lower than in the previous solution, and the maximum is close to 3 s$^{-1}$. In spite of the free solvent transfer which is in general slightly faster than the transfer of the anion, the similar kinetic profile shown by them allows a coupling free solvent-anion transfer to be postulated. On the other hand, independently of the anion in the solution, the $H^+$ ion transfer shows a higher transfer (between 0.2 and 0.1 s$^{-1}$) at the potentials of the "links" process whereas the $H^+$ ion transfer has values lower than 0.1 s$^{-1}$ at the potentials of the "rings" process.


dx.doi.org/10.1021/jp2018204 |J. Phys. Chem. C 2011, 115, 11132–11139

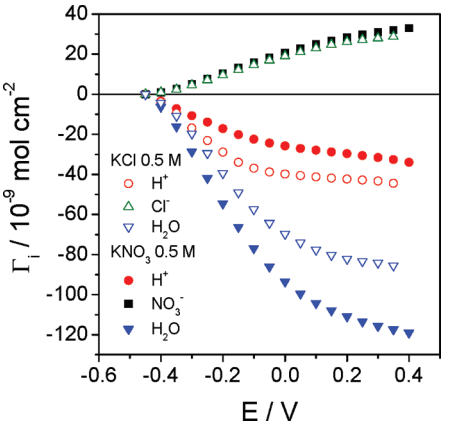


**Figure 6.** Variation of the global insertion law for all the involved species with respect to the potential $KNO_3$ 0.5 M (filled symbols) and KCl 0.5 M (open symbols) solutions at pH = 5 obtained by integrating of $Gi/K'_i$ obtained by fitting $\Delta q/\Delta E(\omega)$ and $\Delta m/\Delta E(\omega)$ with the theoretical functions, eqs 7 and 8, respectively.

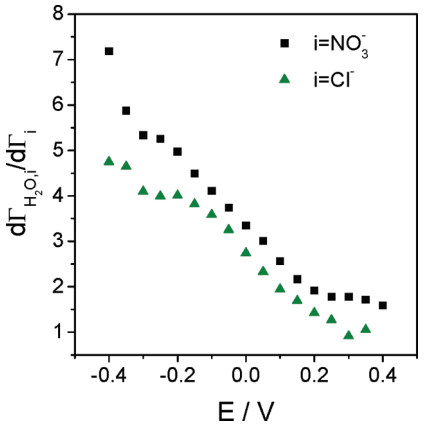


**Figure 7.** Variation of the ratio $d\Gamma_{H_2O,NO_3^-}(E)/d\Gamma_{NO_3^-}(E)$ and $d\Gamma_{H_2O,Cl^-}(E)/d\Gamma_{Cl^-}(E)$ as an estimation of the number of water molecules which are associated with the transfer of the anions in $KNO_3$ 0.5 M (■) and KCl 0.5 M (▲) solutions at pH = 5 obtained by fitting $\Delta q/\Delta E(\omega)$ and $\Delta m/\Delta E(\omega)$ using the theoretical functions, eqs 7 and 8, respectively.

The $d_fG_i/K_i$ ratio for each species transfer corresponds to the derivative of the insertion law with respect to the potential, $d_f(dC_i(E)/dE)$.[34,54] As $d_f$ is unknown, this function is expressed as the derivative of the surface insertion law with respect to the potential, $d\Gamma_i(E)/dE$, where $\Gamma_i$ is the excess surface concentration of the species "$i$". Figure 6 shows the variation of the global insertion law for all the involved species with respect to the potential by integrating the $G_i/K'_i$ ratio. As can be seen, there are two zones clearly separated by a change of slope around 0.0 V. For the "rings" process, the redox reaction is able to insert about $40 \times 10^{-9}$ mol cm$^{-2}$ of the $H^+$ ions in the PAA when $Cl^-$ ions are present in the solution, whereas the amount decreases to about $25 \times 10^{-9}$ mol cm$^{-2}$ in the $NO_3^-$ solution. On the contrary, the amounts of the $H^+$ ions inserted in the $NO_3^-$ solution are about two times more ($10 \times 10^{-9}$ mol cm$^{-2}$) than in the $Cl^-$ solution ($5 \times 10^{-9}$ mol cm$^{-2}$) during the "links" process. In spite of this, the total amount of the $H^+$ ions employed in the redox reactions of the PAA in the $Cl^-$ solution is higher than in the $NO_3^-$ solution.

$\Gamma_{NO_3^-}$ and $\Gamma_{Cl^-}$ have similar values at all potentials; however, the amount of the coupled free solvent is very different. In the presence of the $NO_3^-$ ion about 40% of the amount of water is more transferred than in the $Cl^-$ solution. The ratio $d\Gamma_s(E)/d\Gamma_a(E)$ could be an estimation of the number of inserted/expulsed water molecules per anion of the coupling free solvent−anion transfer. Figure 7 shows the variation of this number with the potential for both the coupling $H_2O-NO_3^-$ transfer, $d\Gamma_{H_2O,NO_3^-}(E)/d\Gamma_{NO_3^-}(E)$, and the coupling $H_2O-Cl^-$transfer, $d\Gamma_{H_2O,Cl^-}(E)/d\Gamma_{Cl^-}(E)$ where $d\Gamma_{i\nu NO_3^-}(E)$ and $d\Gamma_{i\nu Cl^-}(E)$ means the quantity $d\Gamma_i(E)$ in $KNO_3$ and KCl media, respectively. The number of inserted water molecules increases as the PAA is reduced, from 1−2 to 5−6 for anion depending on the anion in the solution. Taking into account that the size of a water molecule may be approximately the difference of size between the two anions, the $NO_3^-$ ion should be able to expel about one molecule of water more than the $Cl^-$ ion as shown in Figure 7.

## 5. DISCUSSION

In the previous works, the insertion/expulsion of anions and protons was postulated for the two electroactive sites identified in the PAA depending on the oxidation state (oxidized, reduced, or intermediate) as the following equations summarize:[46]

$$PAA^{ox}_{link} + e^- \underset{\text{entry of } A^-}{\overset{\text{exit of } A^-}{\rightleftharpoons}} PAA^{*}_{link} \quad (10)$$

$$PAA^{*}_{link} + e^- \underset{\text{exit of } H^+}{\overset{\text{entry of } H^+}{\rightleftharpoons}} PAA^{red}_{link} \quad (11)$$

$$PAA^{ox}_{ring} + e^- \underset{\text{entry of } A^-}{\overset{\text{exit of } A^-}{\rightleftharpoons}} PAA^{*}_{ring} \quad (12)$$

$$PAA^{*}_{ring} + e^- \underset{\text{exit of } H^+}{\overset{\text{entry of } H^+}{\rightleftharpoons}} PAA^{red}_{ring} \quad (13)$$

*ac*-Electrogravimetry allows the ionic transfer of previously postulated reactions to be confirmed, and the behavior of the free solvent during these reactions to be studied as proposed in Figure 8. In addition, the separation in two singular peaks with different formal potentials of the complex shapes of the $G_i$ allows the two electroactive sites and the species transfer to be clearly associated (Figure 4).

As commented above, the fast transfer of the anions seems to be closely coupled with the transfer of the free solvent but in the opposite direction. The water−anion coupled behavior observed in Figure 5 could be due to an exclusion effect.[58] So, the quantity of water depends on the transfer of the anions necessary to compensate the charge of the PAA.[59,60] However, the slightly faster kinetics for the free solvent than for the anions could be influenced by small structural changes of the PAA: when the structure of any site (link or ring) is a double bond and is reduced to single bond, the polymeric chain could get certain degrees of freedom (relaxation of molecular structure).[61] Subsequently, the lattice could carry out a rearrangement in an attempt to balance the charge of the formed polarons (intermediate species) favoring the expulsion of anions by electrostatic repulsion (eq 10 and 12). The exit of the anions from the polymer leaves vacancies which can be occupied by the incoming free solvent molecules. This lattice rearrangement may favor the movement of free

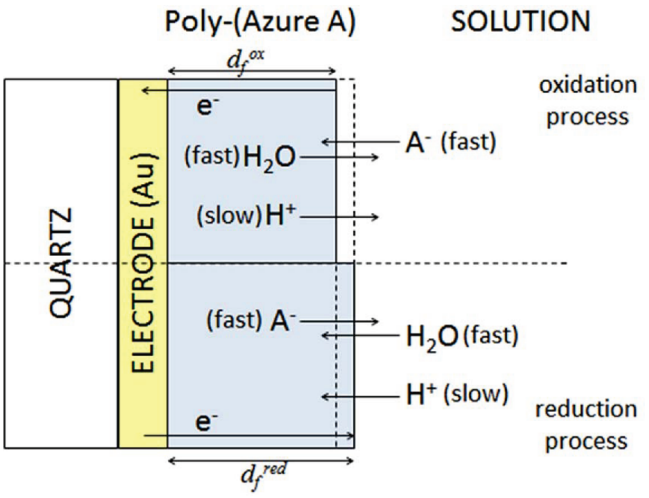


**Figure 8.** Scheme of the "electrode/electroactive polymer/solution" system proposed during the oxidation and reduction of the electrochemical sites in the PAA. $d_f^{ox}$ corresponds to the thickness of the PAA completely oxidized, and $d_f^{red}$, completely reduced.

solvent by increasing the $K'_{H_2O}$ values. In the reverse reaction, the single bonds of the electroactive sites are oxidized to double bonds and the polymer may be more compacted. During this process, the anions enter inside the polymer for compensating the charge; then, the water molecules are expulsed to the solution. This behavior seems to occur independently of the anion in the solution. However, $K'_{H_2O}$ is affected by the size of the coupled anion. As it can be seen in Figure 5, the kinetics of the anion and free solvent in the $KNO_3$ solution is faster than in the KCl solution. This result is in contradiction with the expected kinetics since the smaller anion should be faster than the bigger. However, if the $Cl^-$ ions are really faster than the $NO_3^-$ ions, as expected, but with a depth of insertion inside the polymer much larger for the smallest anion, the apparent value of $K'_{Cl^-}$ could be lower than the apparent value of $K_{NO_3^-}$. In this manner, $d_f$ in $K'_i = K_i/d_f$ should be considered as the insertion depth of the species "$i$" in the polymer.

The transfer of anions and free solvent is more important during the redox reactions of the ring compared with the redox reactions of the link (Table 1). This great difference could be influenced by the different molecular structure of the electroactive sites. However, the environment surrounding the electroactive sites changes with the potential, and this fact must also be taken into account. Two environments can be assumed: during the redox reactions of the link, the rings are oxidized (double bond), whereas during the redox reactions of the ring, the links are reduced (single bond). The relaxation of the polymeric structure after the reduction of the links may improve the insertion/expulsion kinetics of the anion and the free solvent by increasing the diameter of the channels inside the polymer.

The differences between the formal potentials of the anion and the water for each electroactive site point to the dependence of water transfer with respect to anion transfer once more time. The maximum of $G_{H_2O}$ is only reached at more negative potentials than $G_a$ in both sites and solutions. The formal potentials between the anion and the free solvent are separated by about 40 mV for the $H_2O-Cl^-$ couple and by about 70 mV for the $H_2O-NO_3^-$ couple in the two sites (see formal potentials in Table 1). Assuming an exclusion effect and as the water molecules are not implied in the compensation of charge, the highest free solvent transfer only is reached when the polymer has specific physical characteristics: a partial oxidation of the electroactive site and, therefore, a partial amount of vacancies generated for the expelled anions from the polymer. For that reason, the number of water molecules per transferred anion increases when the anion is bigger, when the PAA is reducing and most of the inner anions are out of the polymer (Figure 7). Accordingly, the polymer can be more or less hydrated depending on the oxidation state and the anion in the solution. The steric impediment offered by the transfer of the anions and the molecular structure of the polymer may be the main causes that influence the water transfer directly. In addition, the formation of polarons (intermediate species) inside the polymer for both sites (eqs 10 and 12) may be the origin of the interactions between redox sites causing values of $B_i$ lower than the theoretical ones for these species (Table 1). Besides steric impediments, these charges formed inside the polymer during the redox processes should affect directly the kinetic transfer of anions and, in this manner, indirectly the kinetic transfer of water.

The slow transfer occurring at the two electroactive sites of PAA is associated with the $H^+$ ions. Two reasons lead us to consider $H^+$ ions instead of the $H_3O^+$ ions or $K^+$ ions as a good assumption for the slow process. First, if $\delta_{H_3O^+}m_{H_3O^+} = -19$ g mol$^{-1}$ or $\delta_{K^+}m_{K^+} = -39$ g mol$^{-1}$ is introduced in eq 8 instead of $\delta_{H^+}m_{H^+}$, the fitting procedure leads to bad adjustments at low frequencies. Second, the $H^+$ ions play an important role in the protonation/deprotonation of the molecular structure in the reduction/oxidation of both electroactive sites.[45] This fact could decrease significantly the transfer kinetics of this species inside the polymer, $G_{H^+}$ and $K'_{H^+}$. Moreover, this species is possibly able to deepen inside the polymer more than the other species; therefore, the apparent $K'_{H^+}$ is even lower than the $K_{H^+}$ assuming $d_f$ as the insertion depth.

The order of the formal potentials found for charged species ($H^+$ ions and corresponding anions in Table 1) indicate that the redox reactions of the PAA are successive, as postulated in eqs 10−13. The kinetic transfer of the $H^+$ ions is affected by the nature of the ions in the solution, by the applied potential and by the polymer structure (Figure 5). The small size of the $Cl^-$ ions inside the polymer favors the insertion/expulsion of the $H^+$ ions contrary to the $KNO_3$ solution, probably by steric impediments as commented above for water−anion transfer. The proton insertion/expulsion is faster during the redox process of the links in contrast to the anions and free solvent in both solutions. The rearrangement of the polymeric lattice after the partial reduction of the links (eq 10) could favor the transfer of protons in the polymer if an increase of the ionic channel diameter is assumed. In addition, the chemical reactivity of the $H^+$ ions with the intermonomeric links or with the rings can also affect this parameter since the interactions between redox sites are different (Table 1).

## 6. CONCLUSIONS

All these results show the difficulty of understanding the electrochemical processes of this kind of polymer by classical techniques. The deep analysis of *ac*-electrogravimetry results allows the complicated *redox* processes of PAA to be clarified since two electroactive sites are included in the molecular chain with their electroactivity potential range overlapped. In spite of the similar molecular structure of the sites, several kinetic differences were found by this technique. A model where the anion transfer is the fastest process and the proton transfer the

slowest process is proposed, and coherent results are obtained from EIS and MIS results, confirming an assumed hypothesis in previous work. Moreover, the free solvent plays an important role in mass changes of the PAA whose insertion/expulsion transfer is stoichiometrically coupled with the transfer of the anions but in the opposite direction. The polymer would act like a molecular pump favoring the transfer of the molecular species in different manner depending on the oxidation state of the electrochemical sites.

## AUTHOR INFORMATION

### Corresponding Author

*E-mail: jeronimo.agrisuelas@uv.es.

## ACKNOWLEDGMENT

Part of this work was supported by FEDER-CICyT Project CTQ2010-21133/BQU. J.A. acknowledges his position to the Generalitat Valenciana.

## REFERENCES

(1) Inzelt, G.; Pineri, M.; Schultze, J. W.; Vorotyntsev, M. A. *Electrochim. Acta* **2000**, *45*, 2403–2421.

(2) Inzelt, G. Mechanism of Charge Transport in Polymer Modified Electrodes Electroanalytical Chemistry, A Series of Advances. In *Electroanalytical Chemistry*; Bard, A. J., Ed.; Marcel Dekker, Inc.: New York, 1994; Vol. 18, pp 89−241.

(3) Murray, R. W. Molecular Design of Electrode Surfaces. In *Techniques of Chemistry*; Murray, R. W., Ed.; Wiley: New York, 1992; Vol. 22.

(4) Lyons, M. E. G. *Electroactive Polymer Electrochemistry, Part 1*; Lyons, M. E. G., Ed.; Plenum Press: New York, 1994.

(5) Lyons, M. E. G. *Electroactive Polymer Electrochemistry, Part 2*; Lyons, M. E. G., Ed.; Plenum Press: New York, 1996.

(6) Forster, R. J.; Vos, J. G. *Comprehensive Analytical Chemistry*; Elsevier: Amsterdam, 1992; Vol. 27.

(7) Kulesza, P. J.; Vorotyntsev, M. A. Electrochemistry of Electroactive Materials. In *Electrochimica Acta*; Kulesza, P. J., Vorotyntsev, M. A., Eds.; Elsevier: New York, 2001; Vol. 46, p 26.

(8) Forrest, S. R.; Thompson, M. E. *Chem. Rev.* **2007**, *107*, 923–925.

(9) Sonmez, G. *Chem. Commun* **2005**, *42*, 5251–5259.

(10) Mortimer, R. J.; Dyer, A. L.; Reynolds, J. R. *Displays* **2006**, *27*, 2–18.

(11) Bauldreay, J. M.; Archer, M. D. *Electrochim. Acta* **1983**, *28*, 1515–1522.

(12) Baughman, R. H. *Synth. Met.* **1996**, *78*, 339–353.

(13) Ashley, S. *Sci. Am.* **2003**, *289*, 55.

(14) Pei, Q.; Yu, G.; Zhang, C.; Yang, Y.; Heeger, A. *J. Science* **1995**, *269*, 1086–1088.

(15) Edman, L. *Electrochim. Acta* **2005**, *50*, 3878–3885.

(16) Selvaraju, T.; Ramaraj, R. *Electrochem. Commun.* **2003**, *5*, 667–672.

(17) Wang, Y.; Hu, S. *Biosens. Bioelectron.* **2006**, *22*, 10–17.

(18) Brett, C. M. A.; Inzelt, G.; Kertesz, V. *Anal. Chim. Acta* **1999**, *385*, 119–123.

(19) Karyakin, A. A.; Karyakina, E. E.; Schuhmann, W.; Schmidt, H.-L. *Electroanalysis* **1999**, *11*, 553–557.

(20) Karyakin, A. A.; Bobrova, O. A.; Karyakina, E. E. *J. Electroanal. Chem.* **1995**, *399*, 179–184.

(21) Karyakin, A. A.; Karyakina, E. E.; Schuhmann, W.; Schmidt, H.-L.; Varfolomeyev, S. D. *Electroanalysis* **1994**, *6*, 821–829.

(22) Chen, S.-M.; Lin, K.-C. *J. Electroanal. Chem.* **2001**, *511*, 101–114.

(23) Moore, C. M.; Minteer, S. D.; Martin, R. S. *Lab Chip* **2005**, *5*, 218–225.

(24) Akers, N. L.; Moore, C. M.; Minteer, S. D. *Electrochim. Acta* **2005**, *50*, 2521–2525.

(25) Kertész, V.; Bácskai, J.; Inzelt, G. *Electrochim. Acta* **1996**, *41*, 2877–2881.

(26) Inzelt, G.; Csahók, E. *Electroanalysis* **1999**, *11*, 744–748.

(27) Komura, T.; Ishihara, M.; Yamaguchi, T.; Takahashi, K. *J. Electroanal. Chem.* **2000**, *493*, 84–92.

(28) Gabrielli, C.; Perrot, H.; Rubin, A.; Pham, M. C.; Piro, B. *Electrochem. Commun.* **2007**, *9*, 2196–2201.

(29) To Thi Kim, L.; Sel, O.; Debiemme-Chouvy, C.; Gabrielli, C.; Laberty-Robert, C.; Perrot, H.; Sanchez, C. *Electrochem. Commun.* **2010**, *12*, 1136–1139.

(30) Rubin, A.; Perrot, H.; Gabrielli, C.; Pham, M. C.; Piro, B. *Electrochim. Acta* **2010**, *55*, 6136–6146.

(31) Gabrielli, C.; García-Jareño, J. J.; Keddam, M.; Perrot, H.; Vicente, F. *J. Phys. Chem. B* **2002**, *106*, 3192–3201.

(32) Agrisuelas, J.; García-Jareño, J. J.; Giménez-Romero, D.; Vicente, F. *J. Phys. Chem. C* **2009**, *113*, 8430–8437.

(33) Agrisuelas, J.; García-Jareño, J. J.; Giménez-Romero, D.; Vicente, F. *J. Phys. Chem. C* **2009**, *113*, 8438–8446.

(34) Gabrielli, C.; García-Jareño, J. J.; Keddam, M.; Perrot, H.; Vicente, F. *J. Phys. Chem. B* **2002**, *106*, 3182–3191.

(35) Gabrielli, C.; Perrot, H. Modeling and Numerical Simulations II. In *Modern Aspects of Electrochemistry*; Schlesinger, M., Ed.; Springer: New York, 2009; Vol. 44, pp 151−238.

(36) García-Jareño, J. J.; Sanmatías, A.; Vicente, F.; Gabrielli, C.; Keddam, M.; Perrot, H. *Electrochim. Acta* **2000**, *45*, 3765–3776.

(37) García-Jareño, J. J.; Giménez-Romero, D.; Vicente, F.; Gabrielli, C.; Keddam, M.; Perrot, H. *J. Phys. Chem. B* **2003**, *107*, 11321–11330.

(38) Torres, R.; Jimenez, Y.; Arnau, A.; Gabrielli, C.; Joiret, S.; Perrot, H.; To, T. K. L.; Wang, X. *Electrochim. Acta* **2010**, *55*, 6308–6312.

(39) Chen, C.; Gao, Y. *Electrochim. Acta* **2007**, *52*, 3143–3148.

(40) Karyakin, A. A.; Karyakina, E. E.; Schmidt, H.-L. *Electroanalysis* **1999**, *11*, 149–155.

(41) Chen, C.; Mu, S. *J. Appl. Polym. Sci.* **2003**, *88*, 1218–1224.

(42) Shan, D.; Mu, S.; Mao, B. *Electroanalysis* **2001**, *13*, 493–498.

(43) Bruckenstein, S.; Wilde, C. P.; Shay, M.; Hillman, A. R. *J. Phys. Chem.* **1990**, *94*, 787–793.

(44) Bruckenstein, S.; Wilde, C. P.; Hillman, A. R. *J. Phys. Chem.* **1990**, *94*, 6458–6464.

(45) Agrisuelas, J.; Gabrielli, C.; García-Jareño, J. J.; Giménez-Romero, D.; Perrot, H.; Vicente, F. *J. Phys. Chem. C* **2007**, *111*, 14230–14237.

(46) Agrisuelas, J.; García-Jareño, J. J.; Giménez-Romero, D.; Vicente, F. *Electrochim. Acta* **2010**, *55*, 6128–6135.

(47) Agrisuelas, J.; Giménez-Romero, D.; García-Jareño, J. J.; Vicente, F. *Electrochem. Commun.* **2006**, *8*, 549–553.

(48) Benito, D.; Gabrielli, C.; García-Jareño, J. J.; Keddam, M.; Perrot, H.; Vicente, F. *Electrochim. Acta* **2003**, *48*, 4039–4048.

(49) Benito, D.; Gabrielli, C.; García-Jareño, J. J.; Keddam, M.; Perrot, H.; Vicente, F. *Electrochem. Commun.* **2002**, *4*, 613–619.

(50) Kim, L. T. T.; Gabrielli, C.; Pailleret, A.; Perrot, H. *Electrochim. Acta.* **2011**, *56*, 3516–3525.

(51) Gabrielli, C.; Takenouti, H.; Haas, O.; Tsukada, A. *J. Electroanal. Chem.* **1991**, *302*, 59–89.

(52) Mathias, M. F.; Haas, O. *J. Phys. Chem.* **1992**, *96*, 3174–3182.

(53) Yang, Z.; Coutinho, D. H.; Sulfstede, R.; Balkus, K. J., Jr.; Ferraris, J. P. *J. Membr. Sci.* **2008**, *313*, 86–90.

(54) Gabrielli, C.; Keddam, M.; Nadi, N.; Perrot, H. *J. Electroanal. Chem.* **2000**, *485*, 101–113.

(55) Inzelt, G.; Csahók, E.; Kertész, V. *Electrochim. Acta* **2001**, *46*, 3955–3962.

(56) Frumkin, A. N.; Damaskin, B. B. Adsorption of Organic Compounds at Electrodes. In *Modern Aspects of Electrochemistry*; Bockris, J. O., Conway, B. E., Eds.; Butterworth: London, 1964; Vol. 3, pp 149−223.

(57) Laviron, E. *J. Electroanal. Chem.* **1979**, *100*, 263–270.

(58) Plieth, W.; Bund, A.; Rammelt, U.; Neudeck, S.; Duc, L. *Electrochim. Acta* **2006**, *51*, 2366–2372.

(59) Hillman, A. R.; Loveday, D. C.; Swann, M. J.; Bruckenstein, S.; Wilde, C. P. *J. Chem. Soc., Faraday Trans.* **1991**, *87*, 2047–2053.

(60) Hillman, A. R.; Loveday, D. C.; Swann, M. J.; Bruckenstein, S.; Wilde, C. P. *Analyst* **1992**, *117*, 1251–1257.

(61) Kertész, V.; Berkel, G. J. V. *Electroanalysis* **2001**, *13*, 1425–1430.